Electronic Supplementary Material (ESI) for RSC Advances.

Electronic Supplementary Information

Smartphone-based kanamycin sensing with ratiometric FRET

Saurabh Umrao[a], Anusha S[a], Vasundhara Jain[a,†], Banani Chakraborty[a] and Rahul Roy[a,b,c] *

a. Department of Chemical Engineering, Indian Institute of Science, Bangalore, 560012, India.
b. Molecular Biophysics Unit, Indian Institute of Science, Bangalore, 560012, India.
c. *Center for Biosystems Science and Engineering, Indian Institute of Science, Bangalore, 560012, India.*
†. *Department of Biotechnology, Indian Institute of Technology, Roorkee, 247667, India.*

**Corresponding author. E-mail: rahulroy@iisc.ac.in; Fax: +91-80-2360-8121; Tel: + 91-80-2293-3115/8*

Supplementary figures

Figure S1

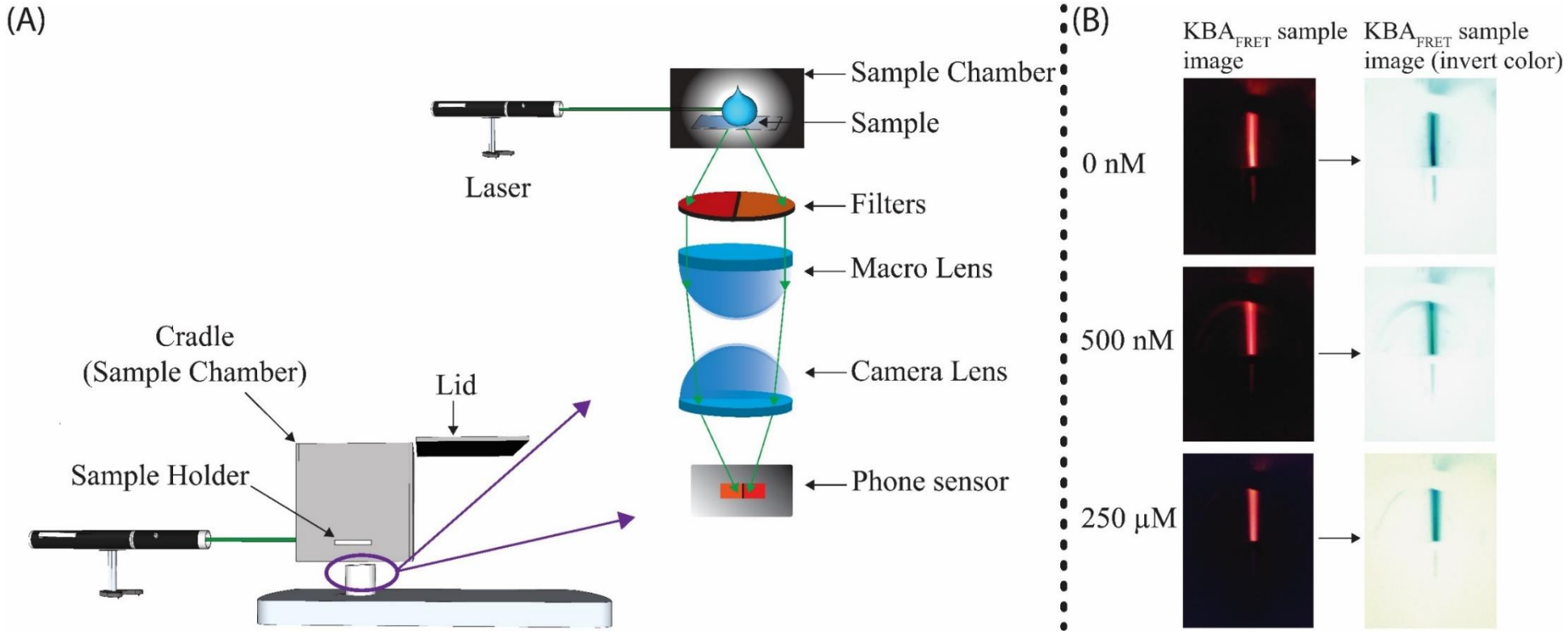

Figure S1: Smartphone-based fluorescence reader setup (A) Schematic of the smartphone setup along with the arrangement of optical components (B) Representative smartphone images acquired at three different concentrations from the custom smartphone setup is depicted. Fluorescence intensity ratio change for KBA_{FRET} with increasing concentrations of kanamycin (0-250 µM) is calculated from the intensity levels in adjacent sections corresponding to different spectral windows as described in methods section.

Figure S2

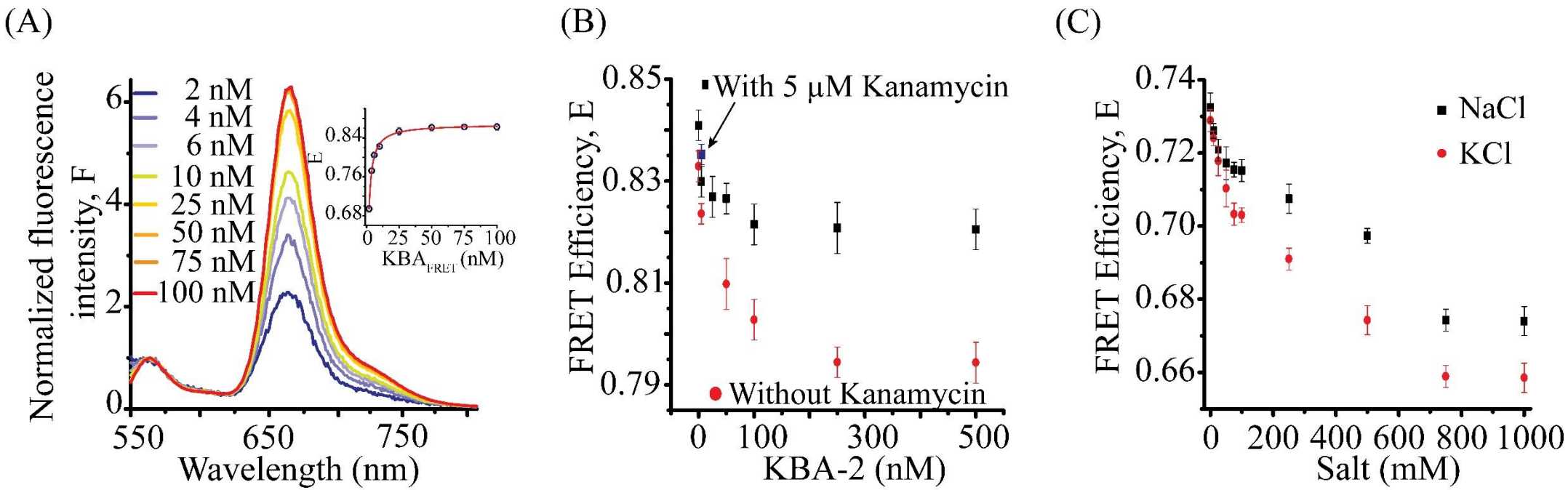

Figure S2: FRET measurement for KBA_{FRET} (A) Fluorescence emission spectra normalized to donor fluorescence amplitude for KBA_{FRET} at different aptamer concentrations. Inset: FRET efficiency change plotted against KBA_{FRET} concentration and fit to the Hill function (line). (B) FRET efficiency change in KBA_{FRET} with titration of unlabelled KBA-2 with and without Kanamycin. (C) FRET efficiency change for KBA_{FRET} with salt titrations.

Figure S3

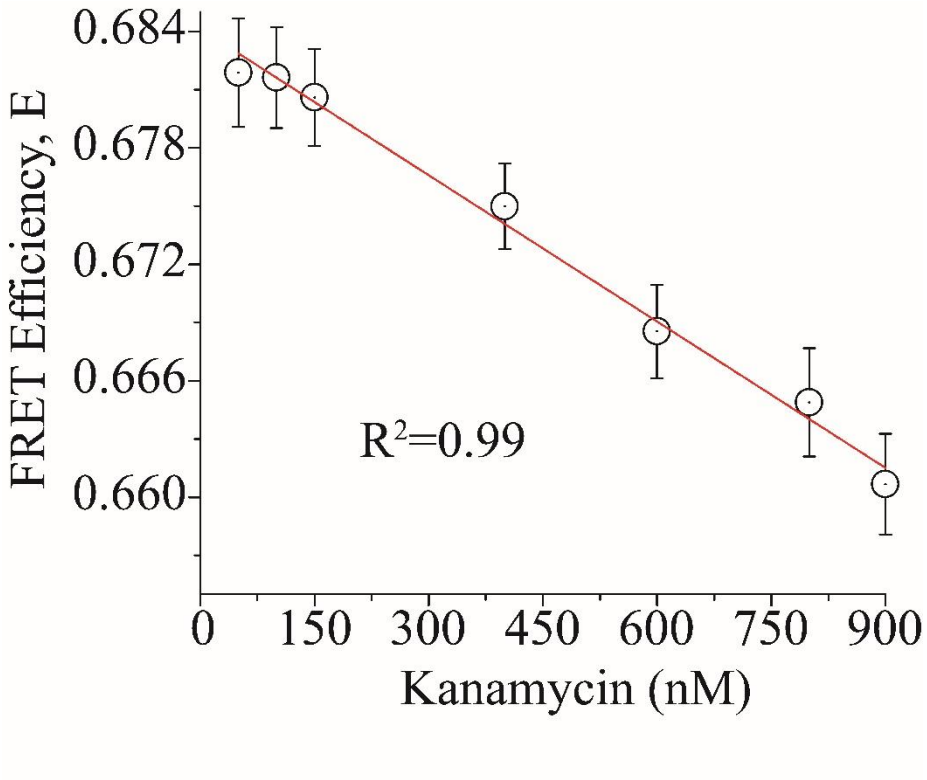

Figure S3: FRET efficiency as function of the kanamycin concentration from 50-900 nM is plotted and fit to the linear plot.

Figure S4

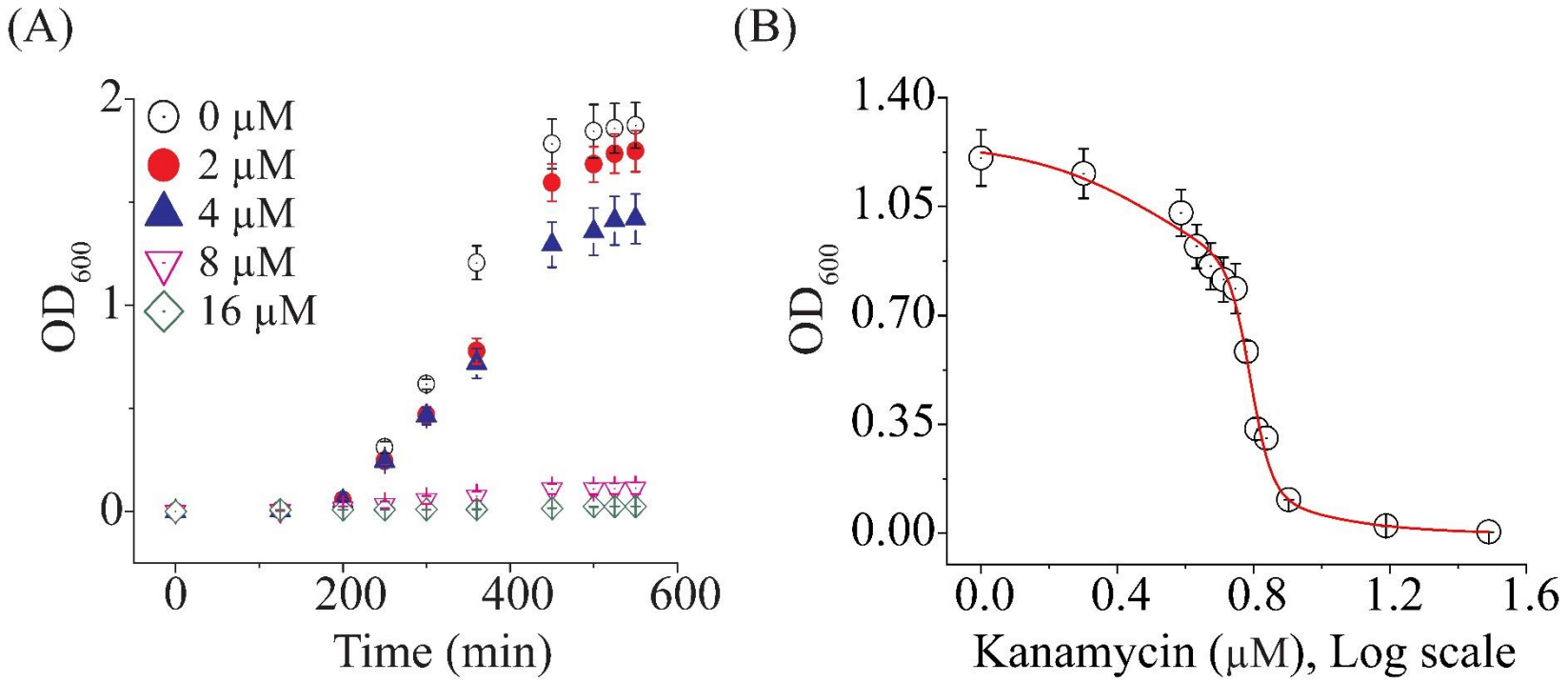

Figure S4: Growth curve of E. coli K-12 in Luria-Bertani (LB) media is plotted as the optical density (OD_{600}) at different kanamycin concentrations. (A) Bacterial cell growth slows down with increasing concentration of kanamycin till beyond. (B) OD_{600} for a range of kanamycin (1-31 μM) at t= 550 mins is plotted. Minimum inhibitory concentration (MIC_{50}) was calculated by fitting the curve using Gompertz model. [57*] All experiments are done at 37°C rotary shaker at 180 rpm speed. We obtained MIC_{50} value of 8.1 μM (4.7 μg/mL), comparable to the reported value of 7.7 μM (4.5 μg/mL) for kanamycin against *E. coli.* [58-59*]

* References are listed in the main text.

Figure S5

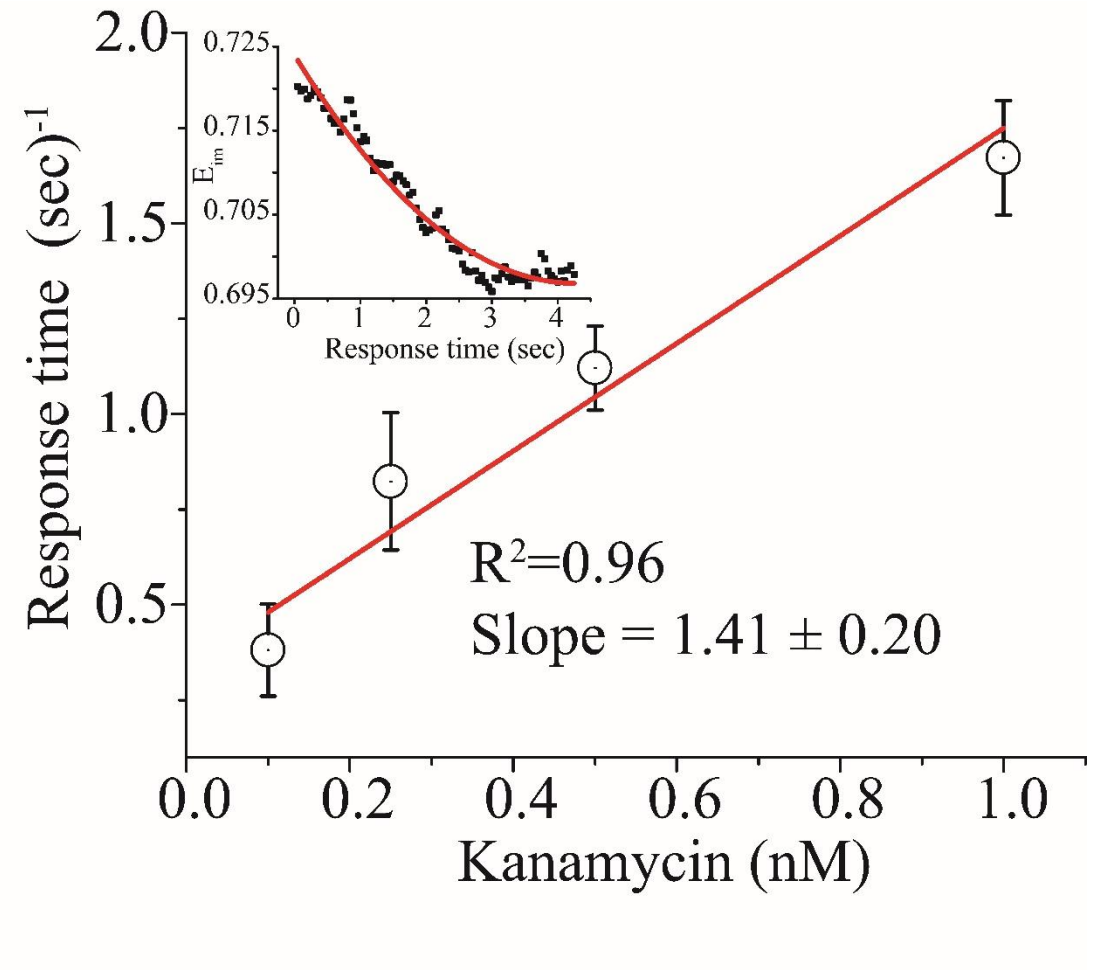

Figure S5: Kanamycin binding with KBA_{FRET} yields a bimolecular association rate constant of (1.41 ± 0.20) x 10^9 $M^{-1}s^{-1}$. Inset: KBA_{FRET} binding with 100 pM kanamycin is rapid and reaches equilibrium within ~ 3 seconds.

Figure S6

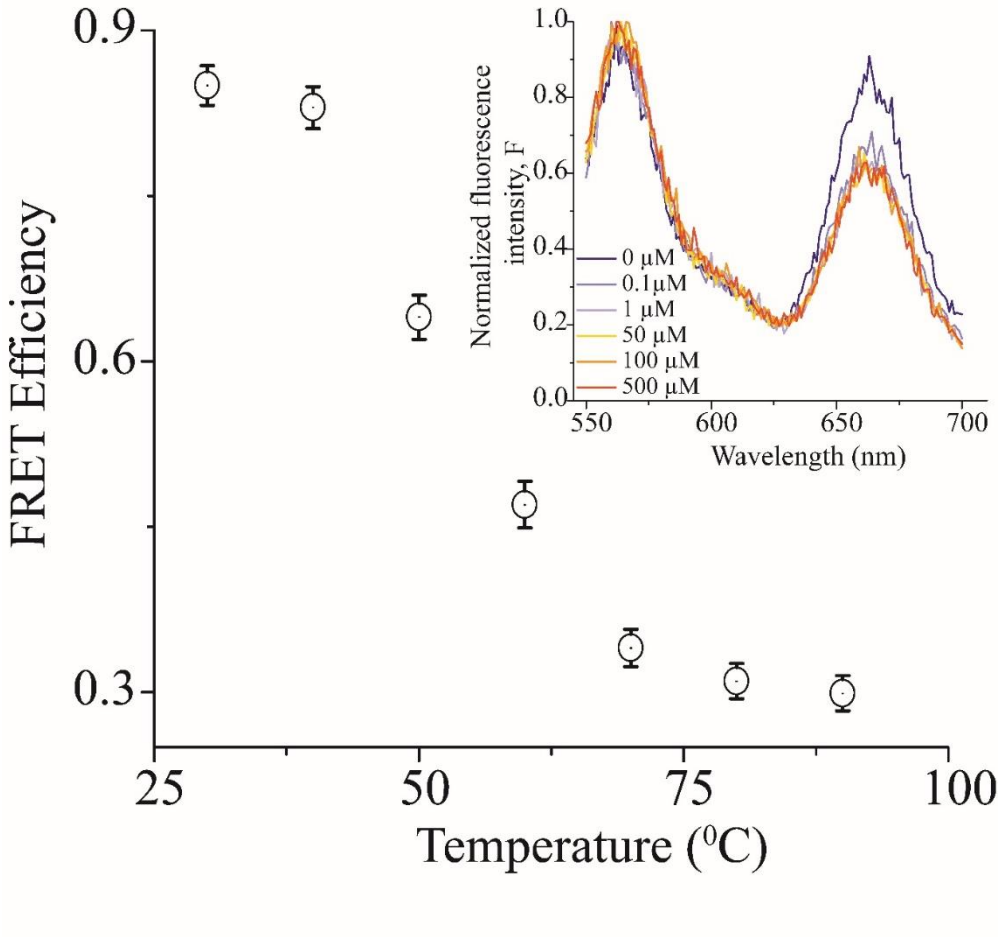

Figure S6: Effect of temperature on KBA_{FRET} construct. Change in FRET efficiency with temperature in absence of kanamycin is plotted. Inset shows the fluorescence change for acceptor emission of KBA_{FRET} as a function of kanamycin concentrations at 60^{o}C.

Supplementary Table S1: Comparison of the proposed method with currently available methods for kanamycin detection.

Methods	Analytical range	LOD	Application to samples	Ref.
Electrochemistry	0.05-9.0 µM	9.4	yes	[1]
Photoelectrochemical	1-230 nM	0.2	no	[2]
Cantilever array	100 µM-10 mM	50,000	no	[3]
Surface plasmon resonance	20-800 nM	2	yes	[4]
Resonance light scattering	10-600 nM	1	yes	[5]
Capillary electrophoresis	0.68-8.5 µM	170	yes	[6]
Spectrophotometry	20-100 nM	9.21	yes	[7]
Colorimetry	-	25	no	[8]
Luminescence	-	143	yes	[9]
Fluorescence	0.5-20 nM	0.32	yes	[10]
Fluorescence	0.1-20 µM	59	yes	[11]
FRET	4-25 µM	1100	yes	[12]
FRET	1 - 20 pM	0.001	yes	[13]*
FRET	0.05 - 5 nM	0.18	yes	this work
$FRET_{smartphone}$	50 - 500 nM	28	yes	this work

* A different aptamer sequence with higher affinity for kanamycin was used.

References:

1. Y. Zhu, P. Chandra, K. M. Song, C. Ban and Y. B. Shim, *Biosensors & Bioelectronics*, 2012, **36**, 29-34.
2. R. Z. Li, Y. Liu, L. Cheng, C. Z. Yang and J. D. Zhang, *Analytical Chemistry*, 2014, **86**, 9372-9375.
3. X. J. Bai, H. Hou, B. L. Zhang and J. L. Tang, *Biosensors & Bioelectronics*, 2014, **56**, 112-116.
4. X. Y. Wang, M. J. Zou, X. Xu, R. Lei, K. A. Li and N. Li, *Analytical and Bioanalytical Chemistry*, 2009, **395**, 2397-2403.
5. C. K. Wang, C. G. Wang, Q. Q. Wang and D. Chen, *Analytical and Bioanalytical Chemistry*, 2017, **409**, 2839-2846.
6. Y. H. Long, A. Hernandez, E. Kaale, A. Van Schepdael, E. Roets, F. Borrull, M. Calull and J. Hoogmartens, *Journal of Chromatography B-Analytical Technologies in the Biomedical and Life Sciences*, 2003, **784**, 255-264.
7. C. S. Wang, J. Liu, X. Y. Han, C. Liu, Y. P. Tian and N. D. Zhou, *Analytical Methods*, 2017, **9**, 4843-4850.
8. K. M. Song, M. Cho, H. Jo, K. Min, S. H. Jeon, T. Kim, M. S. Han, J. K. Ku and C. Ban, *Anal Biochem*, 2011, **415**, 175-181.
9. K. H. Leung, H. Z. He, D. S. H. Chan, W. C. Fu, C. H. Leung and D. L. Ma, *Sensor Actuat B-Chem*, 2013, **177**, 487-492.
10. M. Ramezani, N. M. Danesh, P. Lavaee, K. Abnous and S. M. Taghdisi, *Sensor Actuat B-Chem*, 2016, **222**, 1-7.
11. Y. P. Xing, C. Liu, X. H. Zhou and H. C. Shi, *Scientific Reports*, 2015, **5**.
12. Y. S. Wang, T. C. Ma, S. Y. Ma, Y. J. Liu, Y. P. Tian, R. N. Wang, Y. B. Jiang, D. J. Hou and J. L. Wang, *Microchimica Acta*, 2017, **184**, 203-210.
13. N. R. Ha, I. P. Jung, I. J. La, H. S. Jung and M. Y. Yoon, *Scientific Reports*, 2017, **7**.